Amino-Functionalized Multiple-Walled Carbon Nanotubes-Polyimide Nanocomposite Films Fabricated by *In situ* Polymerization

Yizhe Hu, Liping Wu, Jianfeng Shen, Mingxing Ye

Department of Materials Science, Fudan University, The Key Laboratory of Molecular Engineering of Polymers Ministry of Education, Shanghai, People's Republic of China

Received 30 April 2007; accepted 3 October 2007
DOI 10.1002/app.28644
Published online 9 July 2008 in Wiley InterScience (www.interscience.wiley.com).

ABSTRACT: For the preparation of high-quality polymeric carbon nanocomposites, it is required that carbon nanotubes are fully compatible with matrix polymers. For this purpose, amino-functionalized multiple-walled carbon nanotubes (a-MWNTs) were synthesized. The a-MWNTs/polyimide nanocomposite films were prepared through *in situ* polymerization. According to the spectroscopic characterizations, the a-MWNTs were homogeneously dispersed in the nanocomposite films as the acid-functionalized MWNTs. The mechanical properties of the polyimide composite were also studied.
 J Appl Polym Sci 110: 701–705, 2008

Key words: polyimide composite; amino-functionalized carbon nanotubes; *in situ* polymerization

INTRODUCTION

Since their discovery by Iijima[1] in 1991, multiple-walled and single-walled carbon nanotubes (MWNTs and SWNTs) are of great scientific interest because of their outstanding structural, chemical, electrical, and thermal properties.[2–4] It is believed that the incorporation of carbon nanotubes in polymer matrices endow the composites with many enhanced properties.[5–12] It is a big challenge to have them homogeneously dispersed in desired polymer matrices, given that the carbon nanotubes are generally insoluble and severely bonded. Several approaches have been reported, including the chemical modification of carbon nanotubes[13–16] and the *in situ* polymerization process of polymer with carbon nanotubes.[17,18]

Aromatic polyimides (PI) are high-performance polymers, particularly for its good dielectric properties, superior thermal stability, high strength, low color, flexibility, and processiblity. Therefore, aromatic polyimides are now widely used in a variety of areas, especially in electronic industry and aerospace engineering. Nanocomposites of polyimides with carbon nanotubes are considered to have a promising future in many applications.

To disperse carbon nanotubes into the soluble aromatic polyimide, nanotubes were usually pretreated with acid for the carboxylated functionalization.[18–20] These acid-functionalized carbon nanotubes were well dispersed into the polymer matrix. Here we report a somewhat different approach using amino-functionalized multi-walled carbon nanotubes (a-MWNTs). In this study, we proposed an *in situ* polymerization process of polyimide with a-MWNTs for fabricating composite films. The objective of this study was to develop another method to efficiently disperse carbon nanotubes into a given polymer matrix on a nanoscale level, which lead to a high performance. Results of amino-functionalized MWNTs-polyimide (a-MWNTs/PI) nanocomposite films were also presented and discussed.

EXPERIMENTAL

MWNTs used in this study were purchased from Shenzhen Nanotech Port Co. (Shenzhen, China). The MWNTs produced by the chemical vapor deposition method are averagely 20 nm in diameter (D) and 20–50 μm in length (L). The L/D ratio is 1–2.5 $\times$ 10^3. The diamine 4,4′-oxydianiline (ODA) and the dianhydride 3,3′,4,4′-benzophenone tetracarboxylic dianhydride (BTDA) were dried at 100 and 150°C, respectively, under vacuum prior to use. Dimethylformamide (DMF) was distilled over calcium hydride before use.

Synthesis of amino-functionalized MWNTs

The raw MWNTs were first treated at 530°C in air for 30 min to remove the amorphous carbon

Correspondence to: M. Ye (mxye@fudan.edu.cn).

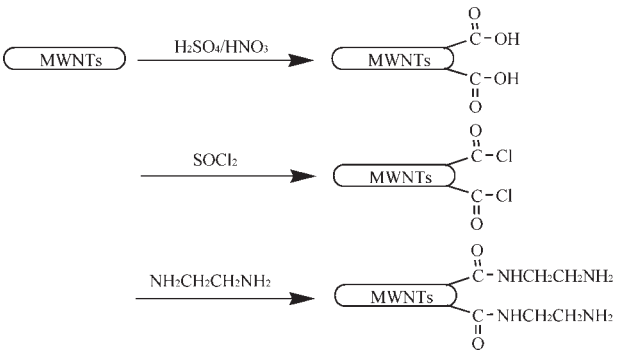

Scheme 1 The strategy for the synthesis of amino-functionalized MWNTs.

followed by being oxidized in a mixture of H_2SO_4 (98%)/HNO_3 (68%) (3 : 1 v/v) at 60°C for 5 h. Then the carboxylated MWNTs were filtered, washed with deionized water until pH was 7, and dried in vacuum. One hundred fifty milligrams of carboxylated MWNTs were stirred in a mixed solvent of $SOCl_2$/DMF (20 : 1, 30 mL) at 70°C for 24 h. The MWNTs were filtered and dried under vacuum after the acyl chlorination. The acyl-chlorinated MWNTs were reacted with 50 mL ethylene diamine at 100°C for 2 days. After cooling to room temperature, the MWNTs were washed with ethanol to remove excessive ethylene diamine. Finally, the black solid was dried in vacuum overnight at room temperature. Corresponding chemical reactions are illustrated in Scheme 1.[21]

Fabrication of the amino-functionalized MWNTs/polyimide composite films

A solution of a-MWNTs in anhydrous DMF was sonicated for 2 h in an ultrasonic bath (50 Hz, SCS1200 Shanghai Qinchao Co.). The solution was then transferred to a three-neck round bottom flask equipped with a mechanical stirrer, nitrogen gas inlet and drying tube outlet filled with anhydrous calcium chloride ($CaCl_2$). Diamine (ODA) was added to the solution, and the mixture was stirred for 30 min. After dianhydride (BTDA) was added, the mixture was stirred overnight under nitrogen at room temperature. Solid content of BTDA-ODA polyamic acid (PAA)-MWNT solution was 10 wt % against DMF. MWNT's content against PAA was 0.1–10 wt %. By casting this solution onto a clean glass, evaporating DMF at 60°C for 4 h, and then step curing (at each temperature of 100, 200, 250, and 300°C for 1 h, respectively), the solvent-free a-MWNTs/PI composite films were obtained.[17,18,22] Scheme 2 shows the fabrication of the a-MWNTs/PI composite films.

Measurements

Functionalization of the nanotubes was confirmed with Raman scattering spectra (Raman, Dilor LAB-

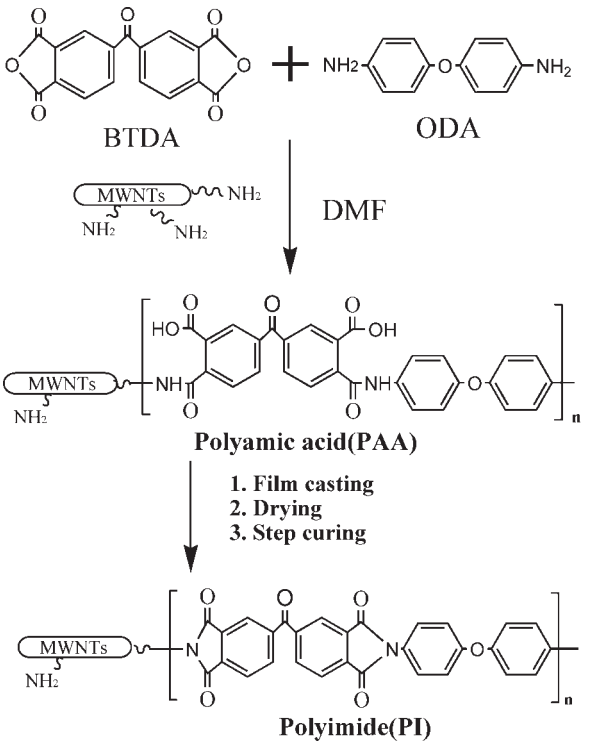

Scheme 2 The fabrication of MWNTs/polyimide composite films.

RAM-1B), X-ray diffraction (XRD, D/max-rB 12 KW) and scanning electron microscopy (SEM, Philips XL30 FEG FE-SEM) analysis. Glass transition temperatures of the films were measured by differential scanning calorimetry (DSC,TA DSC Q100) from 50 to 350°C at a heating rate of 10°C/min. Thermal stability was investigated by dynamic thermogravimetric analysis (TGA, TA TGA Q50) at a heating rate of 10°C/min in air. Dispersion of the MWNTs into the polymer matrix was assessed via Fourier transform infrared spectra (FTIR, NEXUS 670 spectrometer) and SEM (Philips XL30 FEG FE-SEM). Mechanical

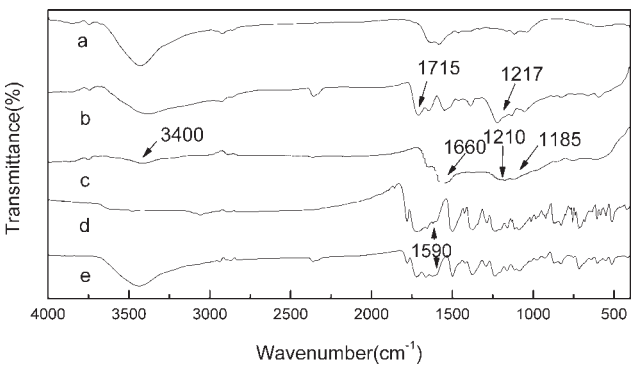

Figure 1 FTIR spectra of (a) raw MWNTs, (b) acid-functionalized MWNTs, (c) amino-functionalized MWNTs, (d) pure polyimide, and (e) the MWNTs/PI nanocomposite containing 1% amino-functionalized MWNTs.

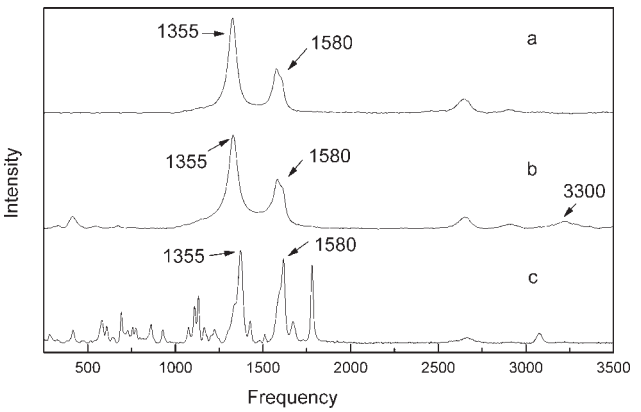

Figure 2 Raman spectra of (a) raw MWNTs, (b) amino-functionalized MWNTs, and (c) the MWNTs/polyimide nanocomposite containing 1% amino-functionalized MWNTs.

properties of the films were evaluated by a dynamic mechanical thermal analyzer (DMA, TA TMA Q800).

RESULTS AND DISCUSSION

Structure of a-MWNTs/PI nanocomposite flims

The FTIR spectra of untreated, acid-functionalized MWNTs and amino-functionalized MWNTs are shown in curves a, b, and c in Figure 1. In spectrum b, the peaks at 1715 and 1217 cm^{-1} correspond to C=O, C—O stretching vibration. In spectrum c, the peaks of C=O, C—O stretching vibration shifted to 1660 and 1204 cm^{-1} due to the formation of amide linkages. The peak at 1185 cm^{-1} is ascribed to C—N stretching of amide groups, while the peak at 3400 cm^{-1} can be assigned to the N—H stretching vibrations.[21] Raman spectroscopy was also employed to probe the amino-functionalization. The Raman spectra in Figure 2 show strong bands at around 1580 cm^{-1} (G mode) which is the Raman-allowed phonon high frequency mode and disordered-induced peak at around 1355 cm^{-1} (D mode), which may originate from the

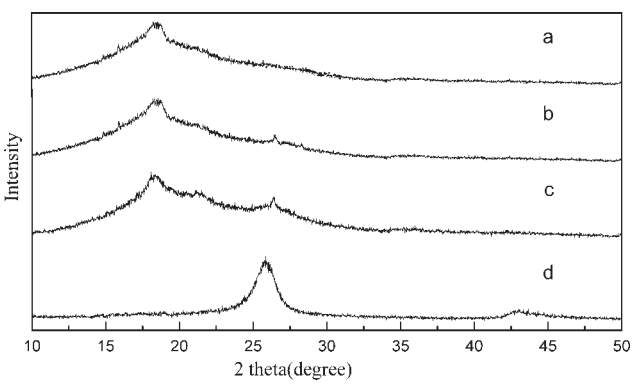

Figure 3 XRD spectra of (a) pure polyimide, (b, c) the MWNTs/polyimide nanocomposite containing 1 and 5 wt % amino-functionalized MWNTs, and (d) amino-functionalized MWNTs.

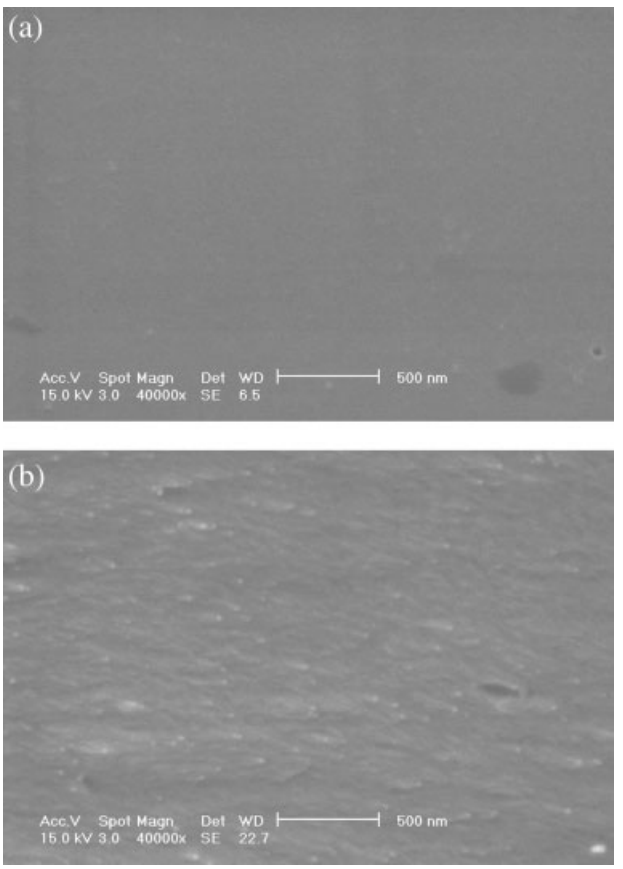

Figure 4 SEM images of (a) BTDA-ODA polyimide and (b) a fracture surface of the 1 wt % a-MWNTS/PI nanocomposite film.

defects in the curved graphene sheets and tube ends.[23] Because of the R—CO—NH—R structure in the amino-functionalized MWNTs, a peak at around 3300 cm^{-1} can be found in spectrum b, which represents the N—H stretching vibrations.[24] Compared with the untreated MWNTs, it is confirmed that the surfaces of the modified MWNTs process the amino groups.

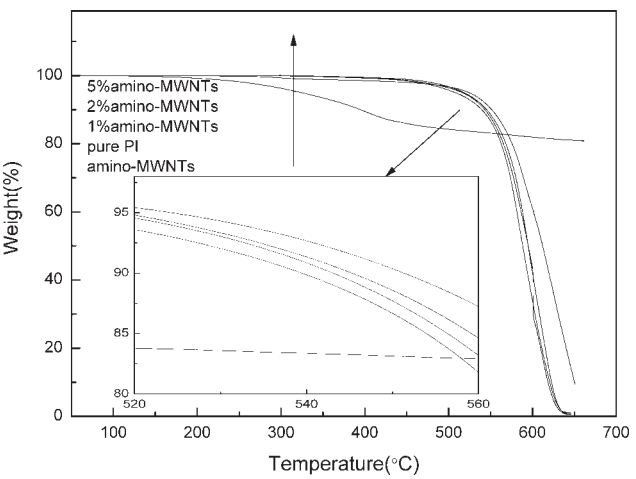

Figure 5 TGA curves of the pure PI, the amino-MWNTs/PI nanocomposites and amino-MWNTs.

TABLE 1
Thermogravimetric Analysis of Pure PI and Amino-MWNTs/PI Nanocomposites

		Amino-MWNTs/PI nanocomposites		
	Pure PI	1 wt %	2 wt %	5 wt %
T_d (°C)	510	518	520	525
T_{d10} (°C)	538	544	546	550

Curve c in Figure 1 shows the peak at around 1590 cm^{-1}, which corresponds to the IR active phonon mode of the MWNTs. Compared with curve d, there is a little enhance in this area in curve e. Because of the strong luminescence of BTDA/ODA, we could not get the Raman spectrum of the pure polyimide. But from the Raman spectrum of amino-MWNTs/polyimide in Figure 2, the characteristic peaks of the a-MWNTs can be found. To further study the structure of the a-MWNTs/PI nanocomposite films, the XRD characterizations of a-MWNTs (curve d), the pure polyimide (curve a), and the a-MWNTs/PI nanocomposite containing 1 and 5 wt % a-MWNTs (curve b and c) were presented in Figure 3. In the case of a-MWNTs, the diffraction peaks at $2\theta = 25.9$ and 43° were observed, corresponding to the interlayer spacing of the nanotube (d_{002}) and the d_{100} reflection of the carbon atoms, respectively. The pure polyimide shows an obvious peak centered at 18.5° corresponding to (110) reflection of BTDA-ODA polyimide.[25] The XRD spectra of the amino-MWNTs/PI nanocomposites show both the characteristic peaks of the pure polyimide and the amino-MWNTs. Traces of diffraction peaks at $2\theta = 25.9°$ were observed as the ratio of amino-MWNTs increased to 1 wt %, indicating that the part of a-MWNTs have not fully interacted with BTDA/ODA molecules. Moreover, the intensity of the peaks assigned to the a-MWNTs in the composite enhanced with the increase of a-MWNTs.[22,23] The microstructure of BTDA-ODA polyimide and the amino-MWNTs/PI nanocomposites investigated by SEM is presented in Figure 4, which shows that the amino-MWNTs (the white dots) were uniformly dispersed throughout the bulk of the polyimide matrix.

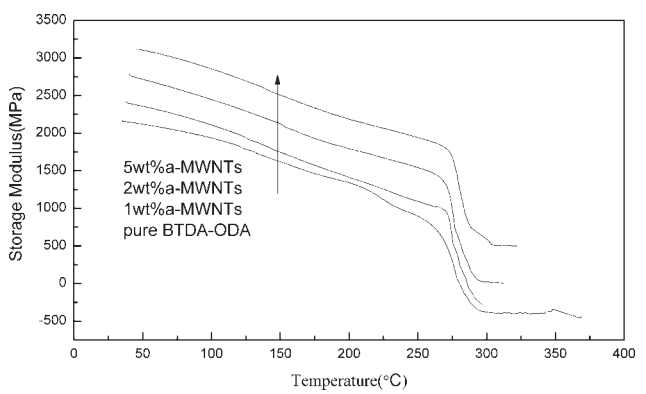

Figure 6 Dynamic mechanical storage moduli for a-MWNTs/PI nanocomposite films.

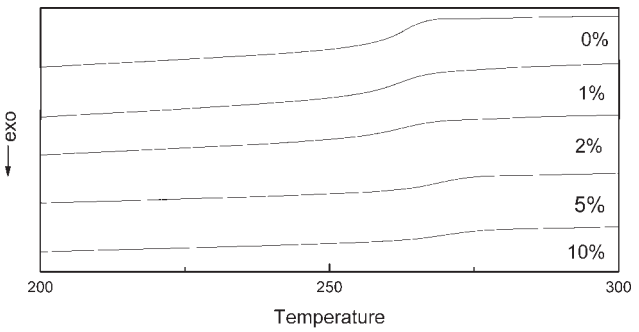

Figure 7 DSC curves for the pure PI and the amino-MWNTs/PI nanocomposites obtained at a heating rate of 10°C/min.

Thermal properties of the a-MWNTs/PI nanocomposites

Figure 5 shows the thermogravimetric profiles of the pure BTDA-ODA polyimide, amino-MWNTs, and the a-MWNTs/PI nanocomposite films. The 5 wt % decomposition temperature (T_d) measured under N_2 is enhanced with the increasing amino-MWNTs content, and shifts from 510°C (pure BTDA-ODA) to 525°C (5 wt % amino-MWNTs), as shown in Table I. The increase in thermal stability of the nanocomposites can be attributed to the chemical bonding in the interphase between the a-MWNTs and the polyimide. The 10 wt % decomposition temperatures (T_{d10}) were also listed in Table I.

Dynamic mechanical properties of the amino-MWNTs/PI nanocomposites

Figure 6 show the DMA of a-MWNTs/PI nanocomposite films. In Figure 6, the storage moduli of a-MWNTs/PI nanocomposite films was enhanced with the increasing a-MWNTs content. Moreover, the a-MWNTs/PI nanocomposite films have a larger storage modulus than pure BTDA-ODA polyimide within the test temperature range.

TABLE 2
Glass Transition Temperatures (T_gs) of Pure PI and Amino-MWNTs/PI Nanocomposites Determined by DSC measurement

		Amino-MWNTs/PI nanocomposites		
	Pure PI	1 wt %	2 wt %	5 wt %
T_g(°C) (by DSC)	262	263	264	268
T_g(°C) (by DMA)	280	286	290	295

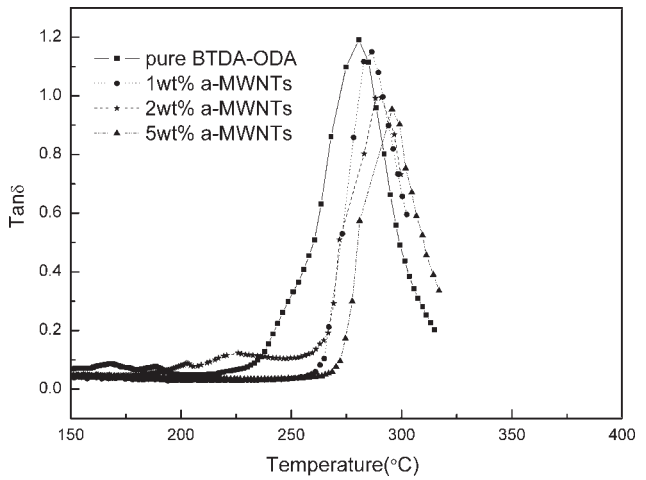

Figure 8 Dynamic mechanical tan δ curves of the a-MWNTs/PI nanocomposite films.

Glass transition behavior

Representative DSC spectra for the pure polyimide and for the nanocomposites with different amino-MWNTs are illustrated in Figure 7. DSC curves for the pure polyimide and the nanocomposites were obtained at a heating rate of 10°C/min. The T_g values of all the specimens were determined from the mid points of the corresponding glass transition regions and were listed in Table II. The increase of the a-MWNTs content results in a shift of T_g to higher temperatures, which is derived from the effect of a-MWNTs on the segmental mobility of polyimide. It can also be showed by the tan δ curves in Figure 8. In the DMA thermograms, the T_g was determined from the maximum of tan δ peak. This phenomenon may be attributed to the chemical bonding and the hydrogen bonding between the a-MWNTs and the polyimide. The T_g values determined by DMA were also listed in Table II.

The T_g obtained from the DMA method appears at a higher temperature than from the DSC method. The T_g difference ranges from 8 to 28°C depending on the specimen and the methodology. The main reason might be the different instrumental mechanisms associated with data acquisition. The DMA method is more sensitive to large-scale molecular motions. The frequency applied in DMA is normally much greater than that in DSC, leading to a shift of the tan δ maximum to a higher level.[26]

CONCLUSIONS

A-MWNTs/PI nanocomposite films were successfully synthesized via *in situ* polymerization. The data from FTIR and Raman spectroscopy, SEM photo, XRD, TGA, DSC, and DMA analysis demonstrated that a-MWNTs were well dispersed in the PI matrix. Compared with the pure BTDA-ODA polyimide, the appearance of a-MWNTs into the polyimide led to an obvious improvement in the thermal and dynamic mechanical properties of the nanocomposite films.

References

1. Iijima, S. Nature 1991, 354, 56.
2. Ajayan, P. M. Chem Rev 1999, 99, 1787.
3. Baughman, R. H.; Zakhidov, A. A.; Heer, W. A. Science 2002, 297, 787.
4. Kovtyukhova, N. I.; Mallouk, T. E.; Pan, L.; Dickey, E. C. J Am Chem Soc 2003, 125, 9761.
5. Chen, R. J.; Zhang, Y.; Wang, D.; Dai, H. J Am Chem Soc 2001, 123, 3838.
6. Star, A.; Stoddart, J. F.; Steuerman, D.; Diehl, M.; Boukai, A.; Wong, E. W.; Yang, X.; Chung, S. W.; Choi, H.; Health, J. R. Angew Chem Int Ed 2001, 40, 1721.
7. Ko, F.; Gogotsi, Y.; Ali, A.; Naguib, N.; Ye, H.; Yang, G.; Li, C.; Willis, P. Adv Mater 2003, 15, 1161.
8. Barrau, S.; Demont, P.; Peigney, A.; Laurent, C.; Lacabanne, C. Macromolecules 2003, 36, 5187.
9. Smith, J. G.; Connell, J. W.; Delozier, D. M.; Lillehei, P. T.; Watson, K. A.; Lin, Y.; Zhou, B.; Sun, Y. P. Polymer 2004, 45, 825.
10. Ge, J. J.; Hou, H.; Li, Q.; Graham, M. J.; Greiner, A.; Reneker, D. H.; Harris, F. W.; Cheng, S. Z. D. J Am Chem Soc 2004, 126, 15754.
11. Hill, D.; Lin, Y.; Qu, L.; et al. Macromolecules 2005, 38, 7670.
12. Zhou, B.; Lin, Y.; Hill, D. E. Wang, W.; et al. Polymer 2006, 5323.
13. Delozier, D. M.; Watson, K. A.; Smith, J. G.; et al. Macromolecules 2006, 1731.
14. Shigeta, M.; Komatsu, M.; Nakashima, N. Chem Phys Lett 2006, 418, 115.
15. Wise, K. E.; Park, C. E.; Siochi, J.; Harrison, J. S. Chem Phys Lett 2004, 391, 207.
16. Valentini, L.; Puglia, D.; et al. Chem Phys Lett 2005, 403, 385.
17. Park, C.; Ounaies, Z.; Watson, K. A.; et al. Chem Phys Lett 2002, 364, 303.
18. Jiang, X. W.; Bin, Y. Z.; Matsuo, M. Polymer 2005, 46, 7418.
19. Jason, J. G.; Zhang, D.; Li, Q.; et al. J Am Chem Soc 2005, 27, 9984.
20. Qu, L.W.; Lin, Y.; Hill, D. E.; et al. Macromolecules 2004, 7, 6055.
21. Shen, J. F.; Huang, W. S.; Wu, L. P.; Hu, Y. Z.; Ye, M. X. Compos A, 2007, 38, 1331.
22. Zhu, B. K.; Xie, S. H.; Xu, Z. K.; Xu, Y. Y. Compos Sci Technol 2006, 66, 548.
23. Wu, T. M.; Lin, Y. W. Polymer 2006, 47, 3576.
24. Dollish, F. R.; Fateley, W. G.; Bentley, F. F. Characteristic Raman Frequencies of Organic Compounds; Wiley: Newyork, 1974.
25. Ree, M.; Kim, K.; Woo, S. H.; Chang, H. J Appl Phys 1997, 81, 698.
26. Cho, D. W.; Lee, S. Y.; Yang, G. M.; Fukushima, H.; Drzal, L. T. Macromol Mater Eng 2005, 290, 179.